Supporting information:

Intramolecular π-stacked Perylene-Diimide Acceptors for Non-fullerene Organic Solar Cells

Jianquan Zhang,[†,§] Fujin Bai,[§] Yunke Li,[§] Huawei Hu,[#] Bin Liu,[‡] Xinhui Zou,[§] Han Yu,[§] Jiachen Huang,[§] Ding Pan,[‡] Harald Ade,[#,*] He Yan[†,§*]

[†] Hong Kong University of Science and Technology-Shenzhen Research Institute, No. 9 Yuexing 1st RD, Hi-tech Park, Nanshan, Shenzhen 518057, P. R. China

[§] Department of Chemistry and Hong Kong Branch of Chinese National Engineering Research Center for Tissue Restoration & Reconstruction, Hong Kong University of Science and Technology (HKUST), Clear Water Bay, Kowloon, Hong Kong, China

[‡] Department of Physics and Department of Chemistry, Hong Kong University of Science and Technology (HKUST), Clear Water Bay, Kowloon, Hong Kong, China

[#] Department of Physics and Organic and Carbon Electronics Laboratory, North Carolina State University, Raleigh, NC 27695, USA

General Information.

^{1}H and ^{13}C NMR spectra were recorded on a Bruker AV-400 MHz NMR spectrometer. Chemical shifts are reported in parts per million (ppm, δ). ^{1}H NMR and ^{13}C NMR spectra were referenced to tetramethylsilane (0 ppm) for $CDCl_3$. Mass spectra were collected on a MALDI Micro MX mass spectrometer, or an API QSTAR XL System.

Materials. P3TEA,[1] 1,4,5,8-tetrabromonaphthalene (**1**),[2] PDIT,[3] 6,7-dibromonaphthalene-2,3-diyl bis(trifluoromethanesulfonate) (**4**) and 2,3,6,7-tetrabromonaphthalene (**5**) [4] was synthesized according to previous literature. Tetrahydrofuran were freshly distilled before use from sodium using benzophenone as the indicator. All other reagents and chemicals were purchased from commercial sources and used without further purification.

Optical characterizations. Film UV-Vis absorption spectra were acquired on a Perkin Elmer Lambda 20 UV/VIS Spectrophotometer. The films were casted from the solutions of the acceptors with a concentration of 20 mg/mL in 1,2,4-trimethylbenzene. UV-Vis absorption spectra were collected from the solution of two small molecules with the concentration of 1.0×10^{-6} M in chloroform and a cuvette with a stopper (Sigma Z600628) was used to avoid volatilization during the measurement.

Electrochemical characterizations. Cyclic voltammetry was carried out on a CHI610E electrochemical workstation with three electrodes configuration, using Ag/AgCl as the reference electrode, a Pt plate as the counter electrode, and a glassy carbon as the working electrode. 0.1 mol L^{-1} tetrabutylammonium hexafluorophosphate in anhydrous acetonitrile was used as the supporting electrolyte. The materials were drop-casted on the working electrode from a solution with a concentration of 5 mg/mL in toluene. Potentials were referenced to the ferrocenium/ferrocene couple by using ferrocene as external standards in acetonitrile solutions. The scan rate is 0.1 V s^{-1}.

AFM analysis. AFM measurements were performed by using a Scanning Probe MicroscopeDimension 3100 in tapping mode. All film samples were spin-cast on ITO/ZnO substrates.

Solar cell fabrication and testing. Diethylzinc (15 % wt in toluene) and molybdenum trioxide (MoO_3) were purchased from Sigma-Aldrich and used as received without further treatment. Pre-patterned ITO-coated glass substrates were cleaned by sequential sonication in soap deionized water, deionized water, acetone, and isopropanol for 30 min of each step. Active layer solutions (D:A ratio 1:1.5 w/w) were prepared in 1,2,4-trimethylbenzene with 2% 1,8-octanedithiol (polymer concentration: 8.5 mg mL^{-1}). To completely dissolve the polymer, the active layer solution should be stirred on a hotplate at 100 °C for at least 1 hour. Active layers were spin-coated onto the

glass/ITO/ZnO substrates at 100 °C in a N_2 glovebox at 1500-2500 rpm. The optimized active layer thickness was ~110 nm. The active layers were then treated with vacuum to remove the solvent. Subsequently, the blend films were thermally annealed at 100 °C for 5 min before being transferred to the vacuum chamber of a thermal evaporator inside the same glovebox, and a thin layer (7 nm) of MoO_3 was deposited as the anode interlayer, followed by the deposition of 100 nm of Al as the top electrode at a vacuum level of ~1.0×10^{-4} Pa. All devices were encapsulated using epoxy and thin glass slides inside the glovebox. Device *J-V* characteristics were measured under AM 1.5G (100 mW cm^{-2}) using a Newport solar simulator in ambient atmosphere. The light intensity was calibrated using a standard Si diode (with KG5 filter, purchased from PV Measurement) to bring spectral mismatch to unity. *J-V* characteristics were recorded using a Keithley 2400 source meter unit. Typical cells have devices area of 5.9 mm^2, defined by a metal mask with an aperture aligned with the device area. EQEs were measured using an Enlitech QE-S EQE system equipped with a standard Si diode. Monochromatic light was generated from a Newport 300W lamp source.

Hole-mobility measurements. The hole-mobilities were measured using the space charge limited current (SCLC) method, employing a device architecture of ITO/ZnO/blend film/MoO_3/Al. The mobilities were obtained by taking current-voltage curves and fitting the results to a space charge limited form, where the SCLC is described by:

$$J = \frac{9\varepsilon_0\varepsilon_r\mu(V_{appl} - V_{bi} - V_s)^2}{8L^3}$$

Where ε_0 is the permittivity of free space, ε_r is the relative permittivity of the material (assumed to be 3), μ is the hole mobility and L is the thickness of the film. From the plots of $J^{1/2}$ vs $V_{appl} - V_{bi} - V_s$, hole mobilities can be deduced.

Electron mobility measurements. The electron mobilities were measured using the SCLC method, employing a device architecture of ITO/ZnO/blend film/Ca/Al. The mobilities were obtained by taking current-voltage curves and fitting the results to a space charge limited form, where the SCLC is described by:

$$J = \frac{9\varepsilon_0\varepsilon_r\mu(V_{appl} - V_{bi} - V_s)^2}{8L^3}$$

Where ε_0 is the permittivity of free space, ε_r is the relative permittivity of the material (assumed to be 3), μ is the hole mobility and L is the thickness of the film. From the plots of $J^{1/2}$ vs $V_{appl} - V_{bi} - V_s$, electron mobilities can be deduced.

GIWAXS characterization. GIWAXS measurements were performed at beamline 7.3.3 at the Advanced Light Source.[5] Samples were prepared on Si substrates using identical blend solutions as those used in devices. The 10 keV X-ray beam was incident at a grazing angle of 0.11° - 0.15°,

which maximized the scattering intensity from the samples. The scattered X-rays were detected using a Dectris Pilatus 2M photon counting detector. In-plane and out-of-plane sector averages were calculated using the Nika software package.[6] The coherence length was calculated using the Scherrer equation:

$$L_c = \frac{2\pi K}{\Delta q}$$

R-SoXS characterization. R-SoXS transmission measurements were performed at beamline 11.0.1.2 at the Advanced Light Source.[7] Samples for R-SoXS measurement were prepared on a PSS modified Si substrate under the same conditions as those used for device fabrication, and then transferred by floating in water to a 1.5 mm × 1.5 mm, 100 nm thick Si_3N_4 membrane supported by a 5 mm × 5 mm, 200 μm thick Si frame (Norcada Inc.). 2D scattering patterns were collected on an in-vacuum CCD camera (Princeton Instrument PI-MTE). The sample detector distance was calibrated from diffraction peaks of a triblock copolymer poly(isoprene-b-styrene-b-2-vinyl pyridine), which has a known spacing of 391 Å. The beam size at the sample is approximately 100 μm by 200 μm.

Theoretical calculations. All calculations in our work were performed using the Quickstep module of the CP2K program package with a dual basis of Gaussian orbitals and plane waves. The molecularly optimized Gaussian basis sets of double zeta plus polarization quality (DZVP-MOLOPT)[9] were used. The Perdew-Burke-Ernzerhof (PBE)[11] exchange-correlation functional with the van der Waals correction (PBE-D3)[12] and Goedecker-Teter-Hutter (GTH)[10] pseudopotentials were employed. For plane wave grids, we used a finest grid cutoff of 600 Ry and a relative cutoff of 100 Ry. The wavelet based solver was applied to solve the Poisson's equation.[13] The force tolerance is 0.01 eV/Å in the molecular geometry optimization.

Steady state and time-resolved photoluminescence measurements. Photoluminescence (PL) spectra were measured using an Ocean Optics spectrometer, and all samples were spin coated on glass/ITO substrates. The samples were excited with femtosecond laser pulses with a repetition rate of 76 MHz from a Ti:Sapphire oscillator (Coherent Mira 900) at a wavelength of 450 nm. The laser power was adjusted with a neutral density filter and the laser spot size was about 3 mm. The fluorescence spectra were detected with a fiber Ocean Optics spectrometer (USB2000+) and the time-resolved spectra were captured using a Hamamatsu streak camera. The lifetime of PL was fitted using the following equation: $(t) = I_0 e^{-t/\tau} + b$, for which τ is PL lifetime and b is the background intensity due to the instrument noise.

DSC measurement. DSC measurements were performed on a DSC Q1000 V9.7 Build 291 differential scanning calorimeter and standard aluminum sample pans, with a heating rate of 10 °C min^{-1} from room temperature to 350 °C under nitrogen (two heating/cooling cycles). The mass of

samples for measurement is ~2 mg.

Thermal properties.

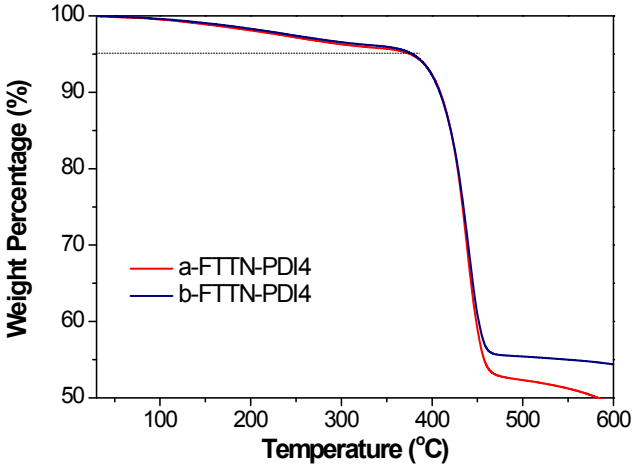

Figure S1. Thermogravimetric curves of a-FTTN-PDI4 and b-FTTN-PDI4. The thermal decomposition temperature are ~375 ℃ (5% weight loss).

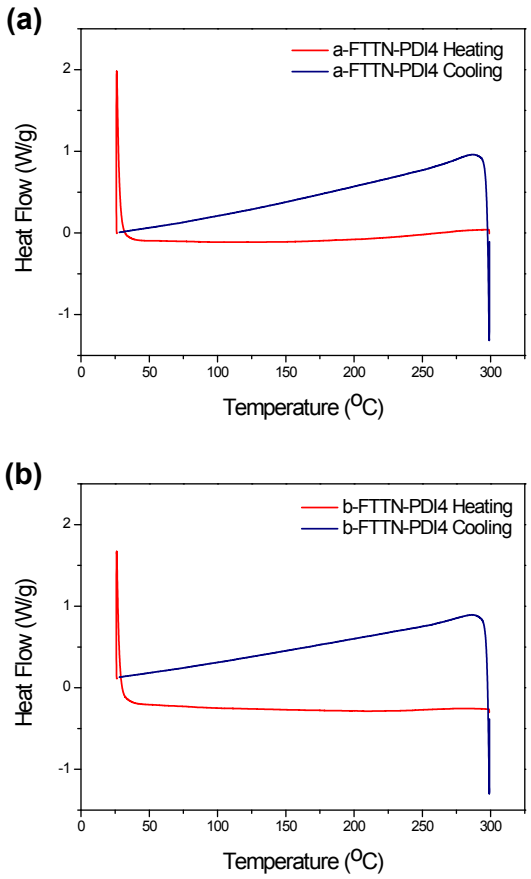

Figure S2. DSC curves of (a) a-FTTN-PDI4 and (b) b-FTTN-PDI4 under N_2 atmosphere with a heating rate of 10 °C/min.

Theoretical calculations.

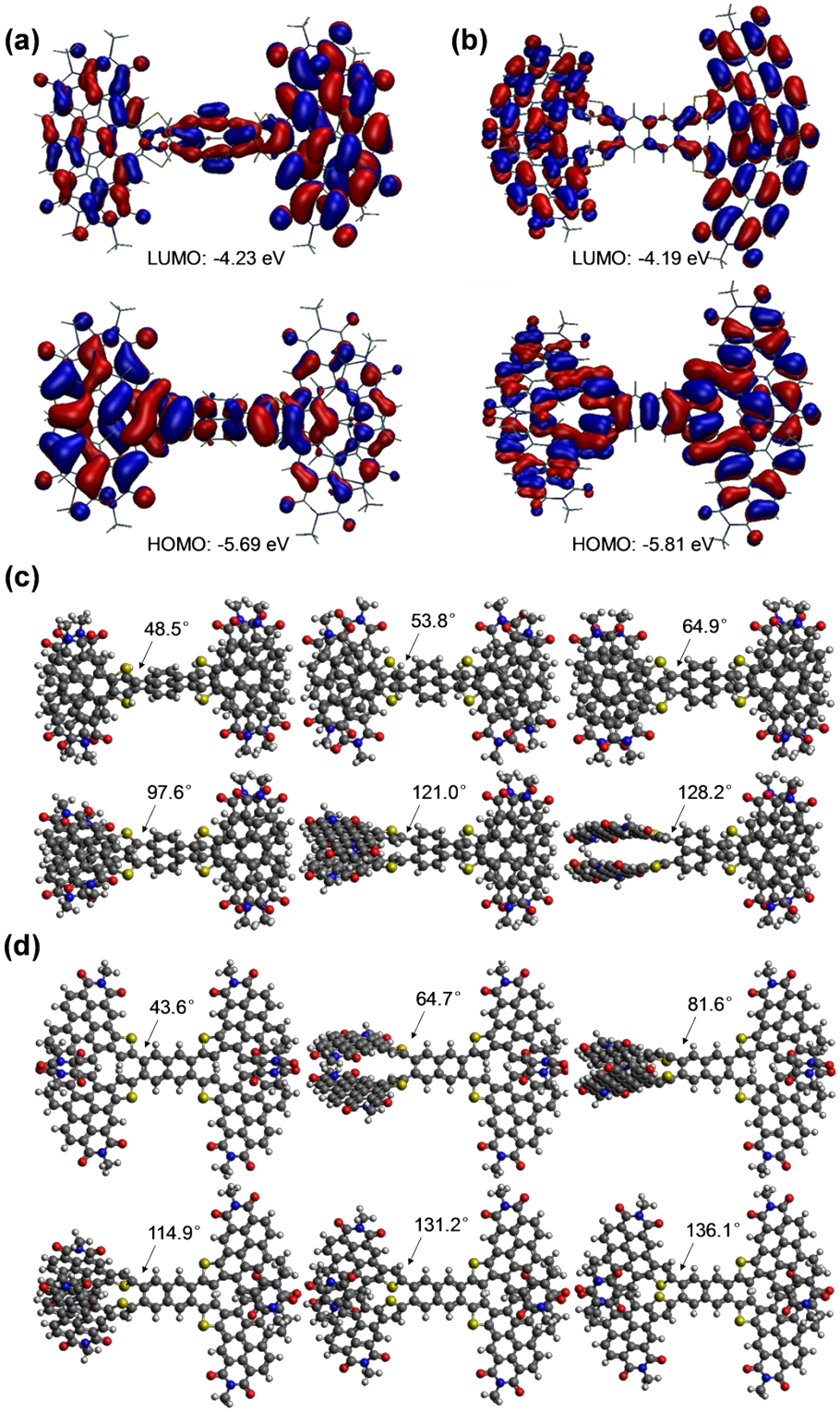

Figure S3. Frontier molecular orbitals of (a) a-FTTN-PDI4 and (b) b-FTTN-PDI4. Optimized geometries obtained from different initial molecular geometries for (c) a-FTTN-PDI4 and (d) b-

FTTN-PDI4.

Optical and electrochemical properties.

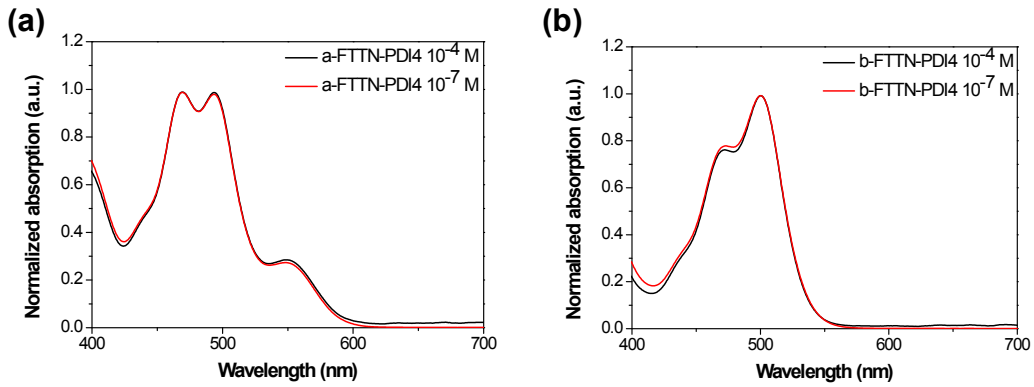

Figure S4. Concentration-variant absorption spectra of the diluted chloroform solution of (a) a-FTTN-PDI4 and (b) b-FTTN-PDI4 with a concentration of 10^{-4} and 10^{-7} M, respectively.

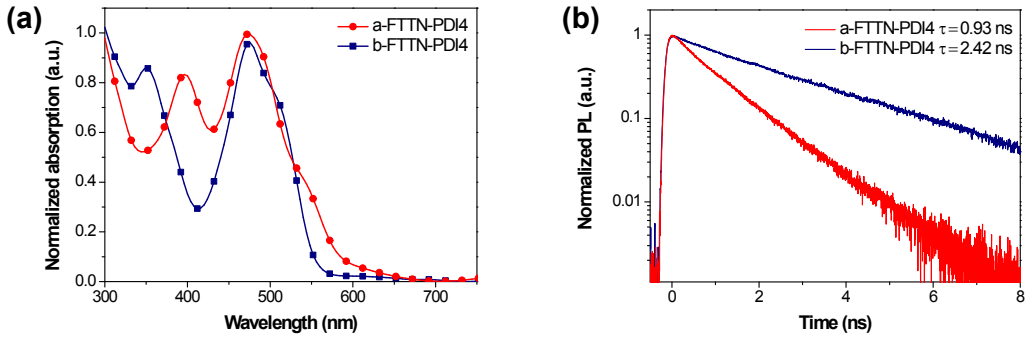

Figure S5. (a) UV-Vis absorption spectra and (b) time-related photoluminescence spectra of the pristine films of a-FTTN-PDI4 and b-FTTN-PDI4.

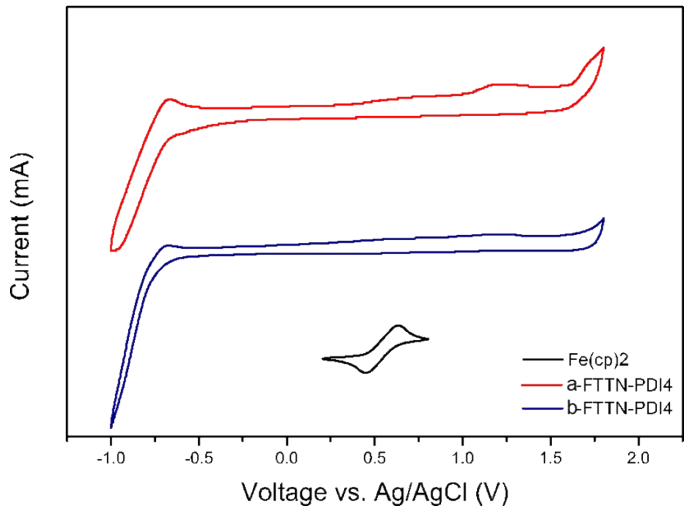

Figure S6. Cyclic voltammetry curves of a-FTTN-PDI4 and b-FTTN-PDI4.

Stability Test.

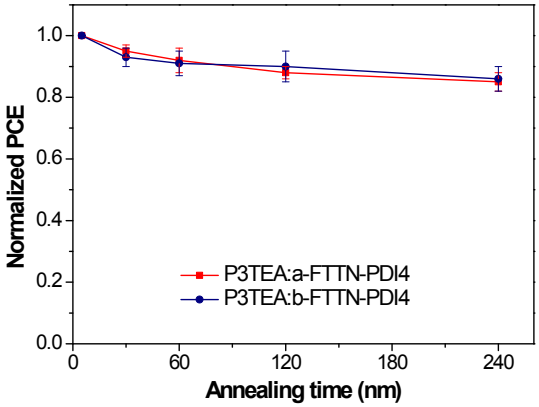

Figure S7. The plot of PCE versus annealing time of the P3TEA:a-FTTN-PDI4 and P3TEA:b-FTTN-PDI4 active layers.

PL experiment.

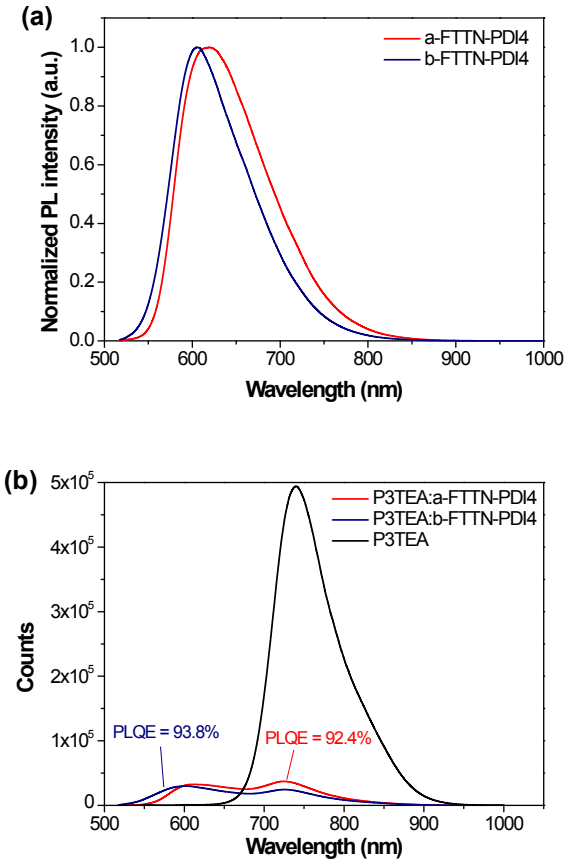

Figure S8. (a) Photoluminescence spectra of the pristine films of a-FTTN-PDI4 and b-FTTN-PDI4.

(b) Photoluminescence quenching experiment of the P3TEA: a-FTTN-PDI4 and P3TEA:b-FTTN-PDI4 blend films relative to the pristine P3TEA film.

Table S1. Device parameters of P3TEA:a-FTTN-PDI4 and P3TEA:b-FTTN-PDI4 under different processing conditions.

	Additive[a]	Thermal annealing[b]	V_{OC} [V]	J_{SC} [mA cm^{-2}]	FF [%]	PCE [%]
P3TEA: a-FTTB-PDI4	N	N	1.12±0.01	9.8±0.2	52±1	5.7±0.3
	N	Y	1.14±0.01	10.3±0.2	55±1	6.5±0.2
	Y	N	1.15±0.01	10.5±0.2	53±2	6.4±0.1
	Y	Y	1.15±0.01	12.0±0.2	61±1	8.4±0.2
P3TEA: b-FTTB-PDI4	N	N	1.13±0.01	8.2±0.2	48±1	4.4±0.2
	N	Y	1.14±0.01	10.2±0.2	52±1	6.0±0.2
	Y	N	1.13±0.01	11.0±0.2	52±1	6.5±0.2
	Y	Y	1.15±0.01	11.5±0.3	55±1	7.2±0.2

[a] 2% ODT.

[b] Thermal annealing at 100^{o}C for 5 mins.

Table S1. Device parameters based on PTB7-Th and PBDB-T with 2% ODT and thermal annealing at 100^{o}C for 5 mins.

Materials	V_{OC} [V]	J_{SC} [mA cm^{-2}]	FF [%]	PCE [%]
PTB7-Th:a-FTTB-PDI4	0.97±0.01	12.1±0.4	58±2	6.8±0.1
PBDB-T:a-FTTB-PDI4	1.03±0.01	9.2±0.3	55±2	5.1±0.2
PTB7-Th:b-FTTB-PDI4	0.96±0.01	13.3±0.2	47±1	6.0±0.1
PBDB-T:b-FTTB-PDI4	1.01±0.01	6.5±0.2	47±1	3.1±0.1

Morphology.

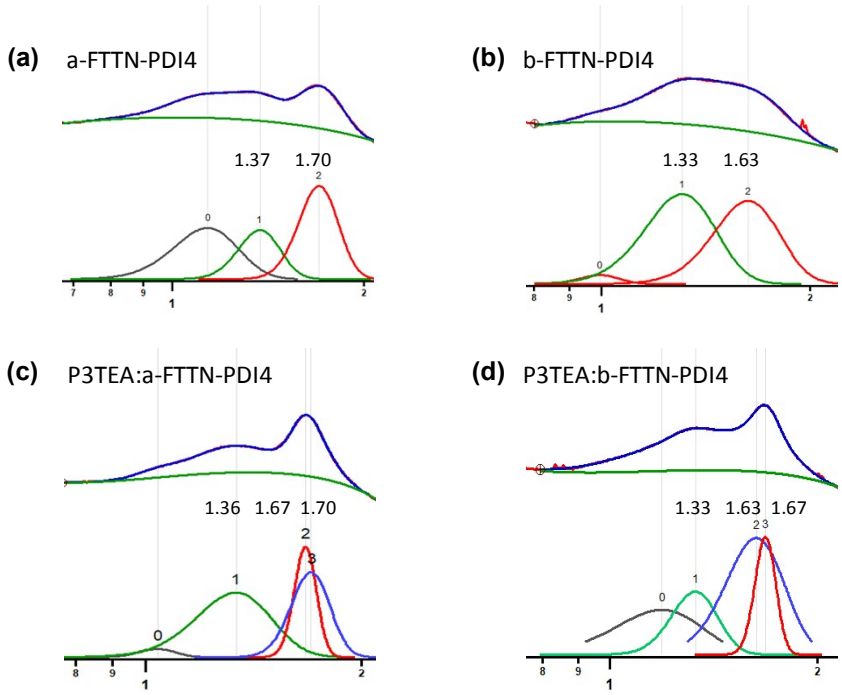

Figure S9. Peak fitting of the π-π stacking peak of (a) a-FTTN-PDI4 and (b) b-FTTN-PDI4 pristine films, (c) P3TEA:a-FTTN-PDI4 and (d) P3TEA:b-FTTN-PDI4 blend film.

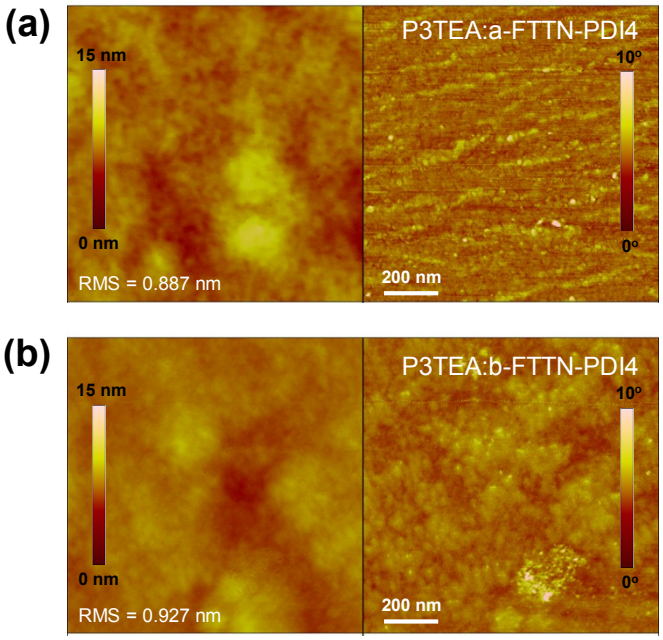

Figure S10. Atomic force microscopy (AFM, left: height image, right: phase image) images of the

blend films of (a) P3TEA:a-TTN-PDI4 and (b) P3TEA:b-FTTN-PDI4.

Charge transport and recombination.

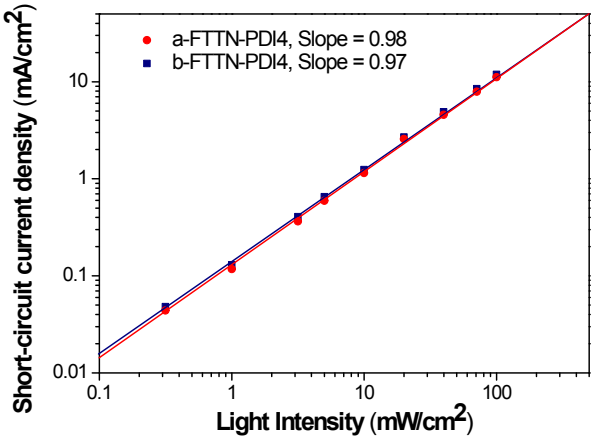

Figure S11. Light-intensity-dependent J_{SC} experiment of P3TEA:a-FTTN-PDI4 and P3TEA:b-TTN-PDI4 and P3TEA:b-FTTN-PDI4.

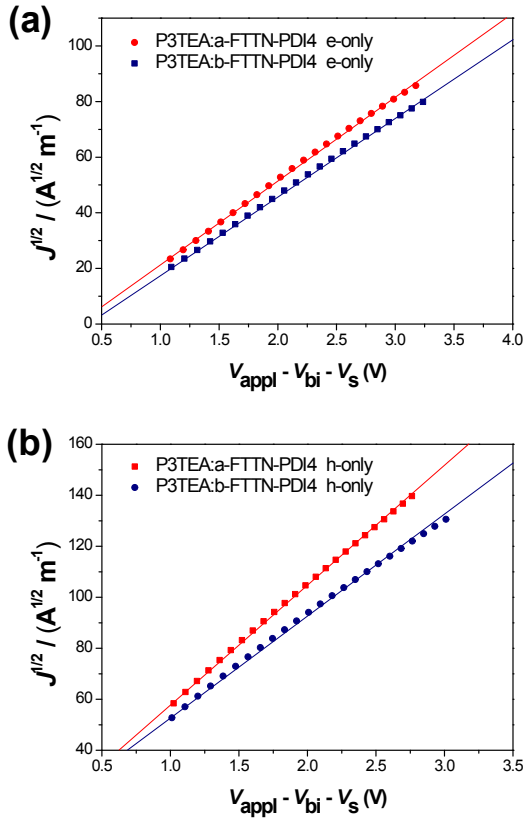

Figure S12. $J^{1/2}$~V characteristics of (a) electron-only devices and (b) hole-only devices of the

P3TEA: a-FTTN-PDI4 and P3TEA:b-FTTN-PDI4 blend films.

Synthesis.

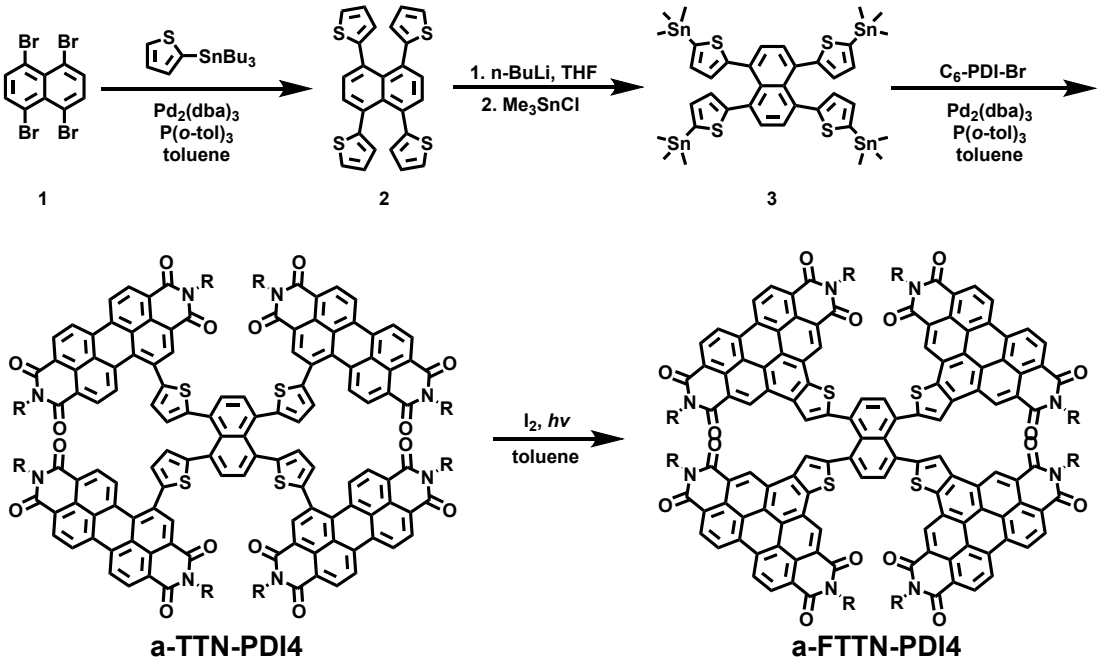

Synthesis of 1,4,5,8-tetra(thiophen-2-yl)naphthalene (2). To a solution of 1,4,5,8-tetrabromonaphthalene (250 mg, 0.563 mmol), $Pd_2(dba)_3$ (52 mg, 0.0563 mmol) and P(*o*-tol)$_3$ (137 mg, 0.0.451 mmol) in toluene (10 mL), 2-(tributylstannyl)thiophene (946 mg, 2.53 mmol) was added under N_2. The reaction mixture was stirred for 12 h at 110 ^oC. Then, the reaction mixture was cooled and poured into an aqueous potassium fluoride. The mixture was extracted with chloroform. The combined organic phase was washed with water followed by brine. Then the solution was dried over Na_2SO_4 and concentrated under reduced pressure. The residue was purified by column chromatography (stationary phase: silica gel; eluent: n-hexane:dichloromethane = 2:1) to get the product as orange solid (185 mg, 72%). ^1H NMR (400 MHz, $CDCl_3$) δ 7.60 (s, 4H), 7.08 (d, J = 4.9 Hz, 4H), 6.73 – 6.65 (m, 4H), 6.60 (d, J = 3.2 Hz, 4H). ^{13}C NMR (101 MHz, $CDCl_3$) δ 144.44, 133.19, 132.60, 130.84, 128.24, 127.04, 124.55. MALDI-TOF MS: Calcd for $C_{26}H_{16}S_4$ (M+): 456.01, Found: 456.01.

Synthesis of 1,4,5,8-tetrakis(5-(trimethylstannyl)thiophen-2-yl)naphthalene (3). To a solution of **2** (100 mg, 0.219 mmol) in anhydrous THF (50 mL) was added n-BuLi (0.55 mL,1.09 mmol, 2 M in hexane) dropwise at -78 ^{o}C under N_2. The mixture was kept at 0 ^{o}C for 1 h and then cooled to -78 ^{o}C again. Trimethyltin chloride (1.3 mL, 1.31 mmol, 1 M in hexane) was added dropwise and the mixture was allowed to react for 2 h. Then, the reaction mixture was poured into aqueous potassium fluoride and extracted with diethyl ether. The combined organic phase was washed with water followed by brine. Then the solution was dried over Na_2SO_4 and concentrated under reduced pressure. The crude product (light yellow solid, 218 mg, 90%) was directly used for the next step without further purification. MALDI-TOF MS: Calcd for $C_{38}H_{48}S_4Sn_4$ (M+): 1111.87, Found: 1111.90.

Synthesis of *a*-TTN-PDI4. To a mixture of **3** (100 mg, 0.0903 mmol), C_6-PDI-Br (301 mg, 0.361 mmol), $Pd_2(dba)_3$ (8 mg, 0.00903 mmol) and P(*o*-tol)$_3$ (22 mg, 0.0722 mmol) in a microwave tube, toluene (5 mL) was added. The reaction was performed by using microwave reactor at 120 ^{o}C. After 2 h, the reaction was stopped and the mixture was extracted by chloroform. The combined organic phase was washed with water followed by brine. Then the solution was dried over Na_2SO_4 and concentrated under reduced pressure. The residue was purified by flash column chromatography (stationary phase: silica gel; eluent: n-hexane: dichloromethane = 2:3) to get the product as dark red solid (234 mg, 75%). ^{1}H NMR (400 MHz, $C_2D_2Cl_4$, 353 K): δ 8.64-8.21 (m, 28H), 7.91 (s, 4H), 7.22 (s, 4H), 7.03 (s, 4H), 5.12-4.80 (m, 8H), 2.14-1.87 (br, 16H), 1.68-1.51 (br, 16H), 1.24-1.10 (m, 128H), 0.83-0.72 (m, 48H). ^{13}C NMR (100 MHz, $CDCl_3$): δ 164.7, 164.5, 163.7, 163.1, 147.3, 144.4, 136.8, 136.1, 134.8, 134.5, 133.5, 133.1, 132.4, 131.7, 130.7, 130.3, 129.9, 129.3, 128.2, 127.5, 126.6, 123.9, 123.4, 123.2, 122.6, 54.7, 32.3, 31.8, 31.7, 29.2, 26.9, 22.6, 14.0, 13.9. MALDI-TOF MS: Calcd for $C_{226}H_{256}N_8O_{16}S_4$ (M+): 3465.83, Found: 3465.88. Elemental Analysis: C, 78.25; H, 7.44; N, 3.23; Found: C, 78.07; H, 7.29; N, 3.51.

Synthesis of *a*-FTTN-PDI4. To a standard photocyclization glassware was added 100 mg of a-TTN-PDI4, 50 ml of toluene and 2 mg of I_2 as catalyst. The mixture was illuminated by 500 W mercury lamp for 2 hours. The solvent was removed under reduced pressure. The crude product was purified by flash column chromatography (stationary phase: silica gel; eluent: n-hexane:

dichloromethane = 1:2) to afford *a*-FTTN-PDI4 as red solid (yield: 91%). ^{1}H NMR (400 MHz, $C_2D_2Cl_4$, 353 K): δ 9.84 (s, 4H), 8.90 (d, 4H, J = 8.0 Hz), 8.79 (d, 4H, J = 8.0 Hz), 8.74 (d, 4H, J = 8.0 Hz), 8.64 (d, 4H, J = 8.0 Hz), 8.44 (s, 4H), 8.24 (s, 4H), 8.13 (s, 4H), 5.40 (m, 4H), 4.94 (m, 4H), 2.61-2.01 (br, 32H), 1.51-1.31 (br, 128H), 0.98-0.72 (br, 48H). ^{13}C NMR (100 MHz, $CDCl_3$): 165.2, 164.8, 164.1, 163.2, 146.2, 138.7, 137.4, 132.8, 131.9, 131.5, 129.0, 128.3, 127.8, 127.2, 126.6, 125.5, 124.8, 124.4, 123.7, 123.0, 122.5, 122.1, 120.7, 120.0, 55.5, 33.4, 32.3, 32.1, 31.8, 30.0, 29.7, 29.3, 29.1, 27.5, 27.0, 22.9, 22.8, 22.6, 14.3. MALDI-TOF MS: Calcd for $C_{226}H_{248}N_8O_{16}S_4$ (M+): 3457.77, Found:3457.84. Elemental Analysis: C, 78.44; H, 7.22; N, 3.24; Found: C, 78.09; H, 7.36; N, 3.44.

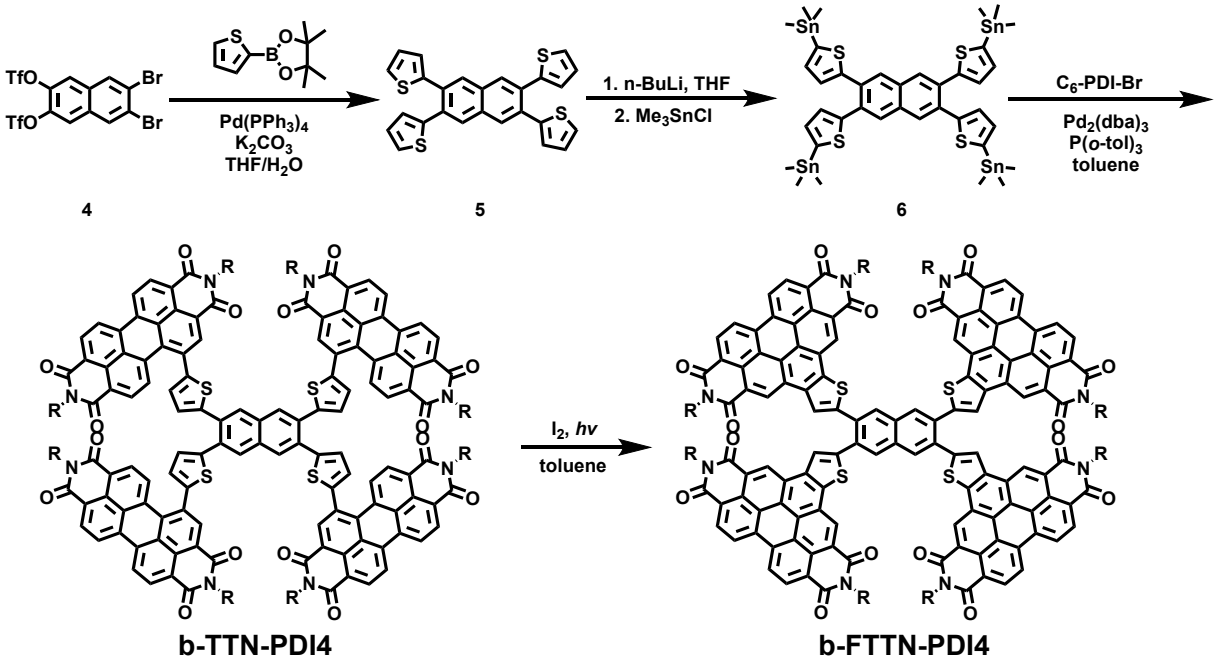

Synthesis of 2,3,6,7-tetrakis(5-(trimethylstannyl)thiophen-2-yl)naphthalene (6). To a solution of **5** (100 mg, 0.219 mmol) in anhydrous THF (50 mL) was added n-BuLi (0.55 mL,1.09 mmol, 2 M in hexane) dropwise at -78 ^{o}C under N_2. The mixture was kept at 0 ^{o}C for 1 h and then cooled to -78 ^{o}C again. Trimethyltin chloride (1.3 mL, 1.31 mmol, 1 M in hexane) was added dropwise and the mixture was allowed to react for 2 h. Then, the reaction mixture was poured into aqueous potassium fluoride and extracted with diethyl ether. The combined organic phase was washed with water followed by brine. Then the solution was dried over Na_2SO_4 and concentrated under reduced

pressure. The crude product (light yellow solid, 201 mg, 83%) was directly used for the next step without further purification. MALDI-TOF MS: Calcd for $C_{38}H_{48}S_4Sn_4$ (M+): 1111.87, Found: 1111.88.

Synthesis of *b*-TTN-PDI4. To a mixture of **6** (100 mg, 0.0903 mmol), C_6-PDI-Br (301 mg, 0.361 mmol), $Pd_2(dba)_3$ (8 mg, 0.00903 mmol) and P(*o*-tol)$_3$ (22 mg, 0.0722 mmol) in a microwave tube, toluene (5 mL) was added. The reaction was performed by using microwave reactor at 120 ^oC. After 2 h, the reaction was stopped and the mixture was extracted by chloroform. The combined organic phase was washed with water followed by brine. Then the solution was dried over Na_2SO_4 and concentrated under reduced pressure. The residue was purified by flash column chromatography (stationary phase: silica gel; eluent: n-hexane: dichloromethane = 2:3) to get the product as dark red solid (215 mg, 69%). ^1H NMR (400 MHz, $C_2D_2Cl_4$, 353 K): δ 8.69-8.59 (m, 20H), 8.50-8.48 (m, 4H), 8.22-8.19 (m, 8H), 7.33 (s, 8H), 5.12-4.96 (m, 8H), 2.16-1.52 (m, 32H), 1.31-1.18 (m, 128H), 0.85-0.79 (m, 48H). ^{13}C NMR (100 MHz, $CDCl_3$): δ 164.6, 163.6, 163.3, 145.1, 144.9, 137.1, 136.5, 135.0, 134.4, 134.3, 133.7, 133.3, 132.2, 132.1, 131.6, 130.7, 129.5, 129.4, 129.1, 129.0, 128.1, 127.5, 127.4, 123.6, 123.1, 122.8, 122.1, 54.8, 32.3, 32.2, 31.7, 31.6, 29.2, 29.1, 26.9, 26.8, 22.6, 22.5, 14.0, 13.9. MALDI-TOF MS: Calcd for $C_{226}H_{256}N_8O_{16}S_4$ (M+): 3465.83, Found: 3465.88. Elemental Analysis: C, 78.25; H, 7.44; N, 3.23; Found: C, 78.37; H, 7.35; N, 3.41.

Synthesis of b-FTTN-PDI4.

To a standard photocyclization glassware was added 100 mg of b-TTN-PDI4, 50 ml of toluene and 2 mg of I_2 as catalyst. The mixture was illuminated by 500 W mercury lamp for 2 hours. The solvent was removed under reduced pressure. The crude product was purified by flash column chromatography (stationary phase: silica gel; eluent: toluene) to afford b-FTTN-PDI4 as red solid (yield: 85%). ^1H NMR (400 MHz, $C_2D_2Cl_4$, 353 K): δ 9.91 (s, 4H), 9.49 (s, 4H), 9.29 (m, 8H), 9.06 (d, 4H, J = 8.0 Hz), 9.01 (d, 4H, J = 8.0 Hz), 8.95 (s, 4H), 8.80 (s, 4H), 5.24-5.16 (m, 8H), 2.25-2.19 (br, 16H), 1.98-1.75 (m, 16H), 1.51-1.17 (m, 128H), 0.82-0.74 (m, 48H). High-quality ^{13}C NMR spectrum were not obtained due to the poor solubility of b-FTTN-PDI4 in $CDCl_3$, $C_2D_2Cl_4$ and C_6D_6. MALDI-TOF MS: Calcd for $C_{226}H_{248}N_8O_{16}S_4$ (M+): 3457.77, Found:3457.84. Elemental

Analysis: C, 78.44; H, 7.22; N, 3.24; Found: C, 78.16; H, 7.47; N, 3.56.

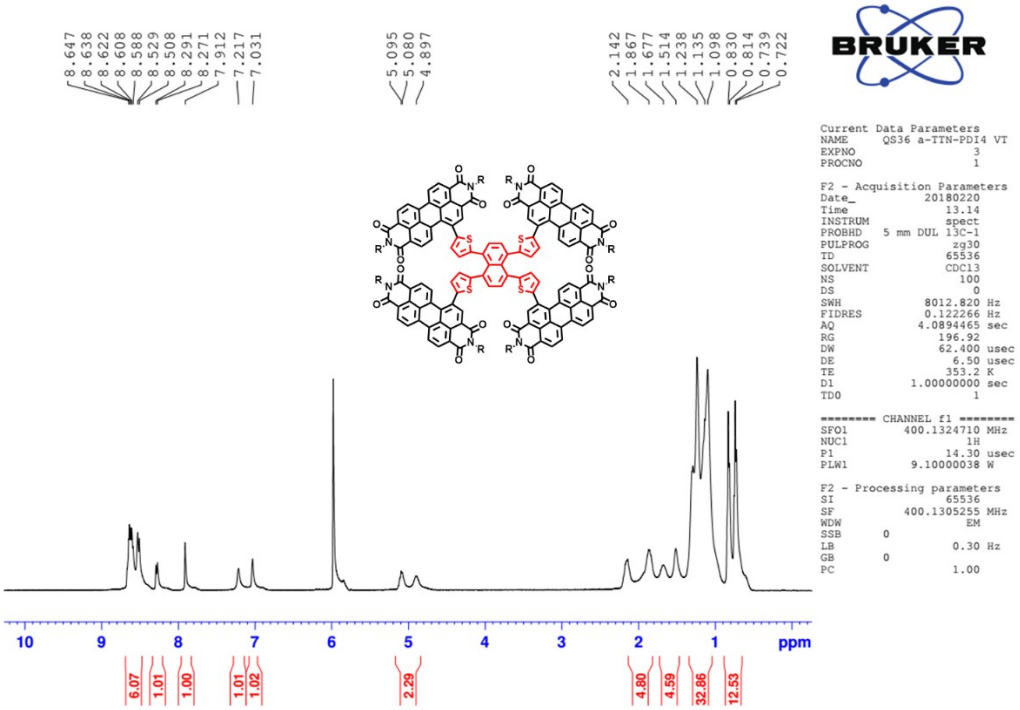

Figure S13. ^{1}H NMR spectrum of a-TTN-PDI4 (400 MHz, $C_2D_2Cl_4$, 353K).

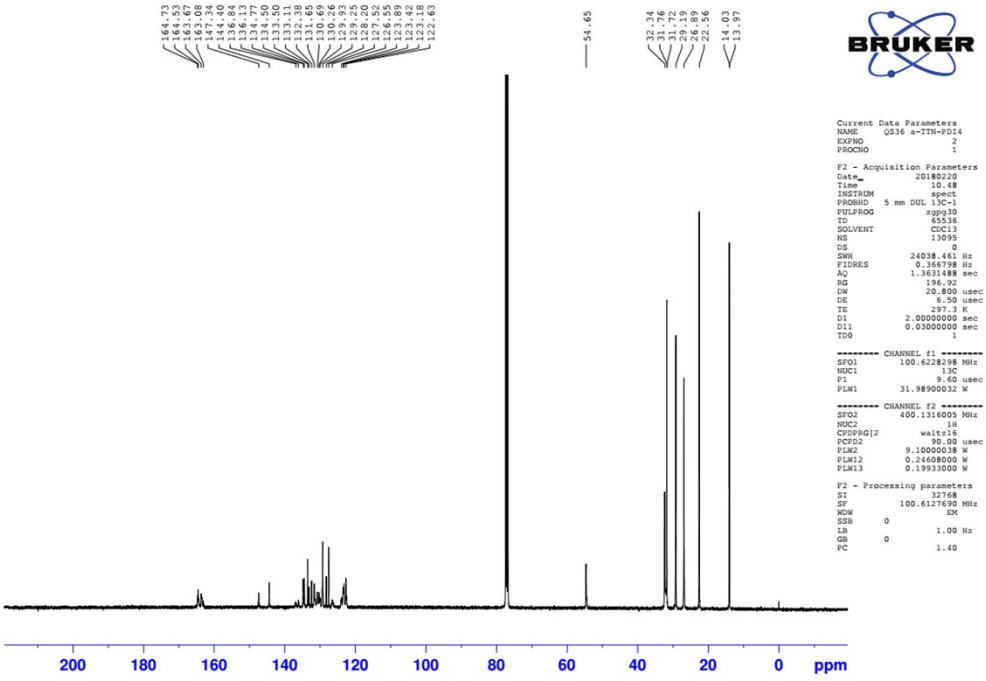

Figure S14. ^{13}C NMR spectrum of a-TTN-PDI4 (100 MHz, $CDCl_3$).

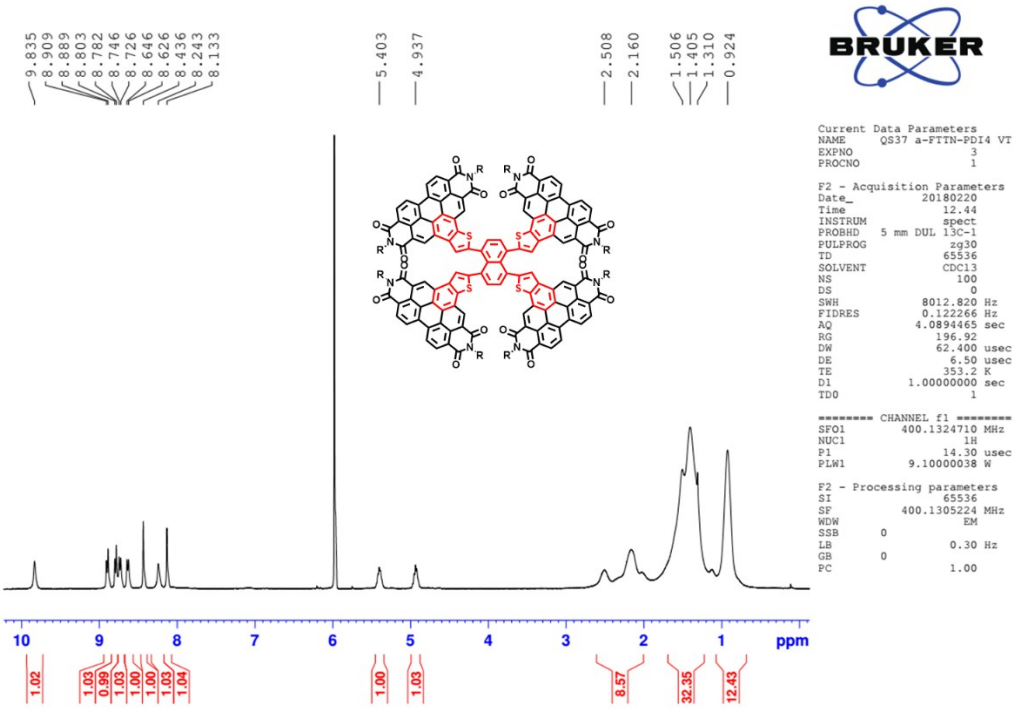

Figure S15. ^{1}H NMR spectrum of a-FTTN-PDI4 (400 MHz, $C_2D_2Cl_4$, 353K).

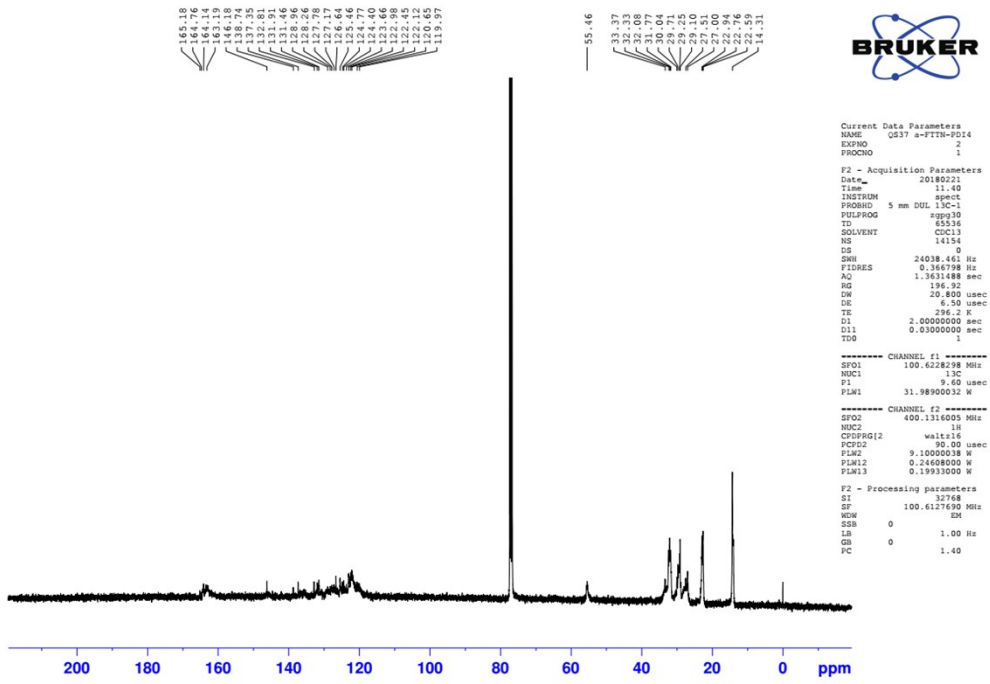

Figure S16. ^{13}C NMR spectrum of a-FTTN-PDI4 (100 MHz, $CDCl_3$).

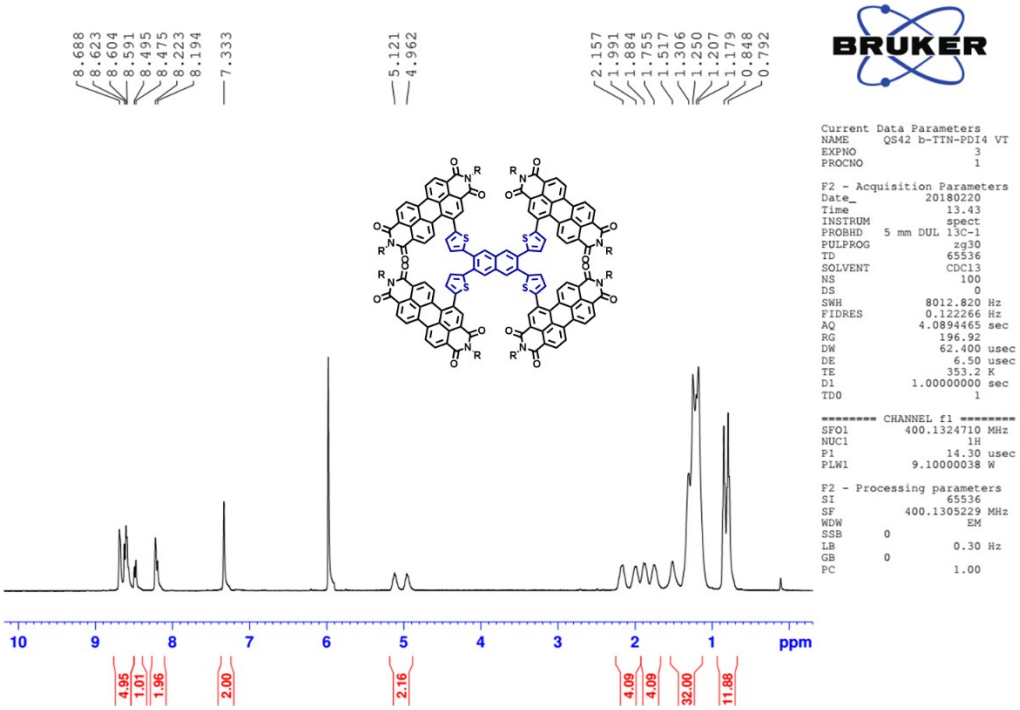

Figure S17. ^{1}H NMR spectrum of b-TTN-PDI4 (400 MHz, $C_2D_2Cl_4$, 353K).

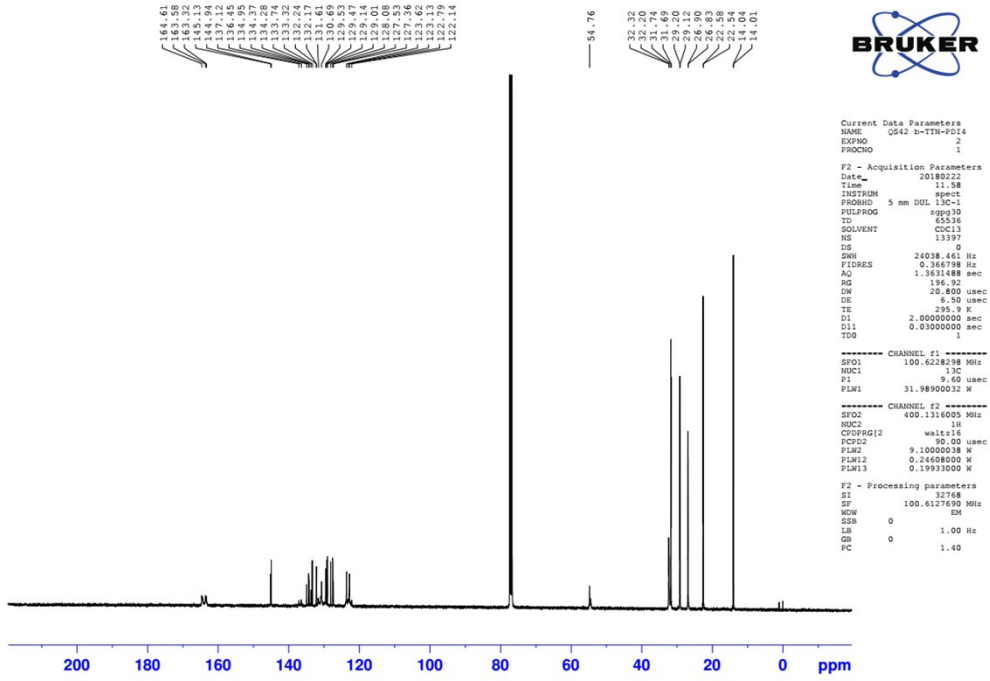

Figure S18. ^{13}C NMR spectrum of b-TTN-PDI4 (100 MHz, $CDCl_3$).

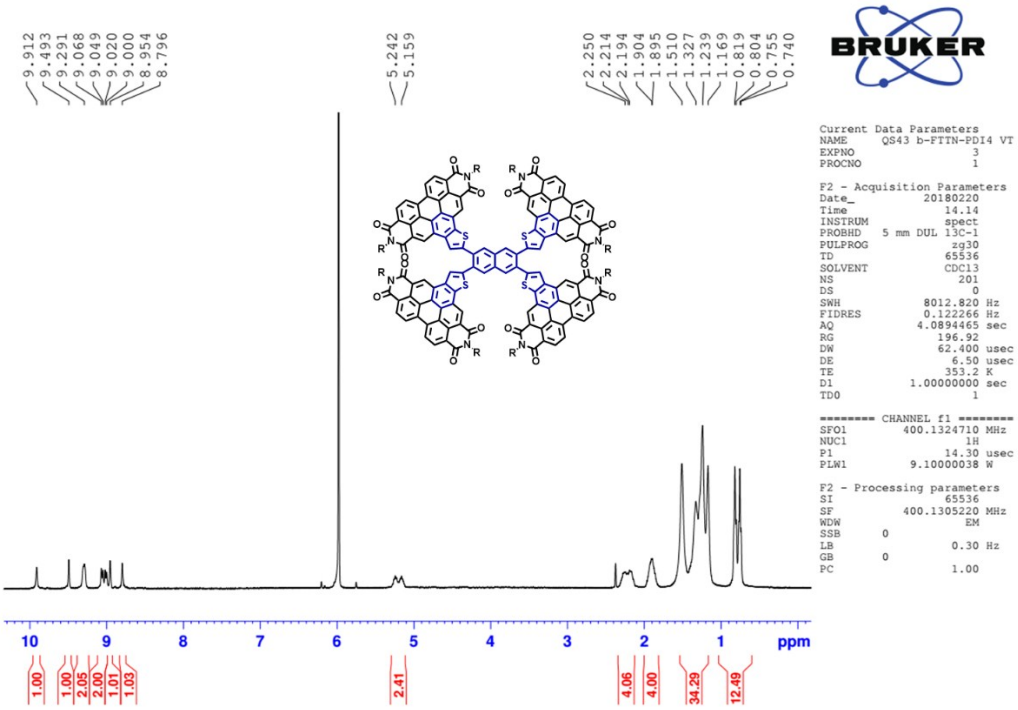

Figure S19. ^{1}H NMR spectrum of b-FTTN-PDI4 (400 MHz, $C_2D_2Cl_4$, 353K).

Cartesian coordinate of the optimized geometry of a-FTTN-PDI4

C	14.30000000	14.68900000	11.00000000
C	13.56500000	13.79600000	11.77200000
C	15.69400000	14.72700000	11.06400000
C	16.40100000	13.84500000	11.87200000
C	14.24700000	12.73600000	12.48100000
C	15.70500000	12.73800000	12.48900000
C	13.56100000	11.67300000	13.18300000
C	14.29100000	10.78300000	13.96300000
C	16.39800000	11.63300000	13.11300000
C	15.68600000	10.74900000	13.91500000
H	13.77200000	15.46300000	10.44300000
H	16.22600000	15.54200000	10.57100000
H	13.76000000	10.00800000	14.51500000
H	16.21500000	9.93600000	14.41400000
C	17.81100000	14.15200000	12.14100000
S	18.91800000	14.47700000	10.82400000
C	20.26500000	14.56400000	11.91500000
C	18.44800000	14.19100000	13.35800000
C	19.85400000	14.39900000	13.25400000
C	21.63300000	14.65100000	11.54000000
C	20.83800000	14.34600000	14.29600000

C	22.61300000	14.58300000	12.57700000
C	22.21600000	14.44300000	13.94500000
H	17.91600000	14.02200000	14.29100000
C	24.00100000	14.59800000	12.23800000
C	25.01000000	14.52500000	13.24800000
C	24.60700000	14.42500000	14.64800000
C	23.21500000	14.35400000	14.96500000
C	22.05000000	14.72400000	10.18600000
C	23.38400000	14.71400000	9.85000000
C	24.38500000	14.65200000	10.86400000
C	26.35800000	14.51100000	12.84400000
C	26.72100000	14.54600000	11.50200000
C	25.74600000	14.60900000	10.50400000
C	23.76200000	14.73500000	8.41800000
C	26.16000000	14.59800000	9.08300000
N	25.13400000	14.73700000	8.12500000
O	22.92800000	14.73700000	7.51000000
O	27.33400000	14.46900000	8.73500000
C	25.50900000	14.77600000	6.70500000
H	25.31900000	13.80700000	6.22500000
H	26.57400000	15.01400000	6.64700000
H	24.90200000	15.53600000	6.20200000
C	20.47800000	14.12100000	15.64800000
C	21.43000000	14.01900000	16.63900000
C	22.81200000	14.16000000	16.32200000
C	25.53600000	14.35700000	15.70200000
C	25.13300000	14.19500000	17.02300000
C	23.77900000	14.07700000	17.34200000
C	20.99300000	13.72600000	18.02800000
C	23.38000000	13.82400000	18.74400000
N	22.00800000	13.67000000	19.00000000
C	21.63700000	13.34300000	20.38100000
H	22.08800000	14.07200000	21.06300000
H	22.01600000	12.34500000	20.63800000
H	20.54700000	13.36200000	20.44800000
O	24.19700000	13.73000000	19.66300000
O	19.81200000	13.53900000	18.32400000
H	21.31900000	14.75900000	9.37800000
H	27.76800000	14.51300000	11.20400000
H	27.14700000	14.44700000	13.59000000
H	26.60300000	14.41100000	15.49500000
H	25.86700000	14.13200000	17.82600000
H	19.43300000	14.00800000	15.93500000
C	23.78000000	11.39900000	7.65700000

C	23.38100000	11.64600000	6.25500000
H	22.08600000	11.38500000	3.93700000
N	22.00800000	11.79700000	5.99800000
C	21.63700000	12.11800000	4.61500000
C	20.99300000	11.74400000	6.97000000
O	19.81200000	11.92900000	6.67400000
H	22.01700000	13.11400000	4.35400000
H	20.54700000	12.10100000	4.54900000
H	27.76800000	11.00400000	13.79800000
C	26.72100000	10.96100000	13.49900000
H	27.14700000	11.06100000	11.41100000
C	26.35800000	10.99100000	12.15600000
H	26.60500000	11.07500000	9.50600000
C	24.38600000	10.83600000	14.13600000
C	25.01100000	10.96700000	11.75200000
C	25.53800000	11.12700000	9.29900000
C	24.00200000	10.88900000	12.76200000
C	24.60800000	11.06200000	10.35300000
H	25.86800000	11.34400000	7.17300000
C	25.13500000	11.28400000	7.97600000
C	22.61300000	10.90000000	12.42300000
C	23.21600000	11.12800000	10.03500000
C	21.63400000	10.83000000	13.46000000
C	22.21800000	11.03900000	11.05500000
C	22.81400000	11.31700000	8.67800000
C	20.26500000	10.91600000	13.08400000
C	20.84000000	11.13300000	10.70300000
C	21.43100000	11.45600000	8.36000000
C	19.85600000	11.08000000	11.74500000
C	20.47900000	11.35400000	9.35100000
H	19.43500000	11.46600000	9.06300000
H	26.57700000	10.45400000	18.35000000
O	27.33100000	11.06100000	16.26500000
C	25.51300000	10.69600000	18.29300000
C	26.15900000	10.90500000	15.91700000
H	25.32900000	11.66600000	18.77500000
N	25.13600000	10.73900000	16.87300000
C	25.74600000	10.88900000	14.49600000
H	24.90300000	9.93900000	18.79500000
C	23.76300000	10.73900000	16.58200000
O	22.93000000	10.72900000	17.49000000
C	23.38500000	10.76600000	15.15000000
C	22.05100000	10.75400000	14.81300000
H	21.32000000	10.71400000	15.62200000

S	18.91500000	11.00200000	14.17300000
C	18.45000000	11.28800000	11.63800000
C	17.81000000	11.32700000	12.85300000
H	17.92000000	11.45600000	10.70400000
O	24.19800000	11.73700000	5.33600000
C	5.88100000	14.80700000	16.68700000
C	6.20700000	14.81600000	18.12900000
H	7.72100000	13.61200000	20.24800000
N	7.56600000	14.74300000	18.47800000
C	7.88200000	14.64400000	19.90700000
C	8.62900000	14.65000000	17.56100000
O	9.79500000	14.53600000	17.94000000
H	7.22000000	15.31300000	20.46500000
H	8.93300000	14.91200000	20.04300000
H	2.23100000	14.33300000	10.33900000
C	3.26000000	14.39300000	10.69100000
H	2.72200000	14.57700000	12.74700000
C	3.55000000	14.53100000	12.04300000
H	3.16000000	14.75900000	14.66500000
C	5.62900000	14.39200000	10.17300000
C	4.87500000	14.59500000	12.51400000
C	4.21400000	14.76700000	14.93500000
C	5.93800000	14.52300000	11.56000000
C	5.19900000	14.69900000	13.93200000
H	3.76900000	14.86100000	17.04900000
C	4.54400000	14.82500000	16.28400000
C	7.30600000	14.55300000	11.97200000
C	6.57200000	14.70300000	14.32900000
C	8.34200000	14.45400000	10.99300000
C	7.62400000	14.63600000	13.36400000
C	6.90000000	14.74600000	15.71800000
C	9.68700000	14.42000000	11.45500000
C	8.98000000	14.61300000	13.80000000
C	8.26400000	14.69300000	16.12500000
C	10.01900000	14.48900000	12.82200000
C	9.26800000	14.63700000	15.18600000
H	10.29500000	14.59000000	15.54400000
H	4.57900000	12.94400000	5.71400000
O	2.79400000	14.00200000	7.92700000
C	4.69600000	14.00200000	5.98300000
C	3.95100000	14.14300000	8.32200000
H	3.75500000	14.52700000	5.79600000
N	5.02500000	14.13500000	7.40900000
C	4.28900000	14.32100000	9.74900000

H	5.51700000	14.43200000	5.40300000
C	6.38100000	14.13600000	7.77300000
O	7.26600000	13.99700000	6.92600000
C	6.68300000	14.30000000	9.21600000
C	7.99800000	14.33300000	9.62200000
H	8.77100000	14.24300000	8.85800000
S	11.10100000	14.15600000	10.47900000
C	11.41600000	14.31700000	13.04700000
C	12.12500000	14.07800000	11.89800000
H	11.89000000	14.32400000	14.02500000
O	5.33800000	14.86300000	19.00300000
C	5.88000000	10.70700000	8.24800000
C	6.20700000	10.69500000	6.80600000
H	7.75100000	11.85900000	4.68400000
N	7.56700000	10.73800000	6.45900000
C	7.88700000	10.82500000	5.02900000
C	8.63000000	10.82800000	7.37600000
O	9.79600000	10.93000000	6.99600000
H	7.20900000	10.17000000	4.47300000
H	8.93000000	10.53100000	4.89500000
H	2.22700000	11.20100000	14.59300000
C	3.25700000	11.13600000	14.24200000
H	2.71900000	10.95200000	12.18600000
C	3.54700000	10.99400000	12.89000000
H	3.15800000	10.78100000	10.26800000
C	5.62500000	11.12500000	14.76200000
C	4.87200000	10.92400000	12.42100000
C	4.21200000	10.76200000	9.99900000
C	5.93400000	10.98900000	13.37500000
C	5.19700000	10.81800000	11.00300000
H	3.76700000	10.67700000	7.88400000
C	4.54200000	10.70300000	8.65000000
C	7.30200000	10.94800000	12.96500000
C	6.57000000	10.80200000	10.60700000
C	8.33700000	11.04000000	13.94400000
C	7.62200000	10.86100000	11.57200000
C	6.89900000	10.75700000	9.21800000
C	9.68300000	11.06200000	13.48500000
C	8.97900000	10.87300000	11.13900000
C	8.26400000	10.79500000	8.81200000
C	10.01700000	10.99200000	12.11800000
C	9.26800000	10.84500000	9.75300000
H	10.29600000	10.88100000	9.39600000
H	4.54300000	12.59400000	19.20700000

O	2.79200000	11.53100000	17.00700000
C	4.68900000	11.53700000	18.94900000
C	3.94900000	11.38700000	16.61200000
H	3.76300000	10.98800000	19.14400000
N	5.02200000	11.39600000	17.52500000
C	4.28500000	11.20400000	15.18500000
H	5.52200000	11.13600000	19.53300000
C	6.37800000	11.38900000	17.16100000
O	7.26500000	11.53300000	18.00600000
C	6.67900000	11.21200000	15.71900000
C	7.99300000	11.16800000	15.31500000
H	8.76700000	11.25600000	16.07900000
S	11.09500000	11.31900000	14.46500000
C	11.41600000	11.15700000	11.89700000
C	12.12300000	11.39200000	13.04900000
H	11.89200000	11.14900000	10.92000000
O	5.33700000	10.66800000	5.93100000

Cartesian coordinate of the optimized geometry of b-FTTN-PDI4

C	18.52200000	16.97800000	16.42700000
C	17.30400000	17.64900000	16.44200000
C	18.52300000	15.53700000	16.24300000
C	17.29800000	14.87900000	16.19200000
C	16.06200000	16.98300000	16.33800000
C	16.06100000	15.55600000	16.26500000
C	14.82200000	17.66600000	16.31500000
C	13.60900000	16.99300000	16.26500000
C	14.82300000	14.87300000	16.24700000
C	13.60900000	15.54400000	16.26300000
C	19.75700000	17.76100000	16.57600000
S	19.90100000	19.29700000	15.74200000
C	21.54900000	19.48000000	16.24800000
C	20.92200000	17.44100000	17.23400000
C	21.97400000	18.37500000	17.01400000
C	22.41500000	20.55600000	15.91000000
C	23.36400000	18.24600000	17.35100000
C	23.78800000	20.44700000	16.28600000
C	24.26400000	19.28200000	16.96900000
H	21.03000000	16.53200000	17.81800000
C	24.69700000	21.49700000	15.95000000

C	26.08800000	21.39800000	16.26500000
C	26.58800000	20.17200000	16.88500000
C	25.66300000	19.13700000	17.22500000
C	21.96600000	21.71200000	15.22300000
C	22.82600000	22.74600000	14.92800000
C	24.20500000	22.66200000	15.28400000
C	26.92200000	22.48400000	15.93600000
C	26.42900000	23.62500000	15.31000000
C	25.07700000	23.72300000	14.97300000
C	22.28900000	23.94300000	14.23000000
C	24.58100000	24.93900000	14.28900000
N	23.21200000	24.97000000	13.95600000
O	21.10600000	24.04300000	13.90800000
O	25.30100000	25.89600000	14.00700000
C	22.74000000	26.17400000	13.26200000
H	23.30700000	26.31000000	12.33300000
H	22.90300000	27.05500000	13.89500000
H	21.67600000	26.04200000	13.05200000
C	23.87300000	17.06400000	17.94200000
C	25.22600000	16.88000000	18.12700000
C	26.14500000	17.91600000	17.78900000
C	27.95600000	19.94900000	17.13600000
C	28.42000000	18.74900000	17.66800000
C	27.52700000	17.72300000	17.98700000
C	25.70300000	15.56400000	18.62000000
C	28.04400000	16.43900000	18.50700000
N	27.09600000	15.42400000	18.75600000
C	27.63300000	14.13300000	19.20100000
H	28.16400000	14.25500000	20.15300000
H	28.34400000	13.75700000	18.45500000
H	26.79200000	13.44500000	19.31400000
O	29.23800000	16.22400000	18.70700000
O	24.93600000	14.63400000	18.87600000
H	20.92100000	21.81600000	14.92800000
H	27.08700000	24.45900000	15.06400000
H	27.98300000	22.44500000	16.17400000
H	28.68600000	20.71700000	16.88700000
H	29.48400000	18.58100000	17.83200000
H	23.21000000	16.24200000	18.20700000
C	27.56800000	14.47700000	15.02300000
C	28.17300000	15.74900000	14.57900000
H	28.41700000	17.92800000	12.91500000
N	27.28900000	16.81300000	14.30600000
C	27.90700000	18.07200000	13.87500000

C	25.88800000	16.75100000	14.41100000
O	25.18400000	17.73400000	14.17300000
H	28.64800000	18.38700000	14.61700000
H	27.11300000	18.81700000	13.77900000
H	26.61400000	7.44300000	16.91600000
C	26.01900000	8.34800000	16.79300000
H	27.69000000	9.57200000	16.28200000
C	26.61300000	9.55400000	16.43600000
H	28.52400000	11.35900000	15.96100000
C	23.84500000	9.42300000	16.84600000
C	25.85700000	10.72700000	16.25000000
C	27.84700000	12.17900000	15.73200000
C	24.44300000	10.65900000	16.44900000
C	26.45600000	11.99900000	15.85400000
H	29.47300000	13.52400000	15.24500000
C	28.39500000	13.39400000	15.33000000
C	23.61300000	11.80200000	16.24100000
C	25.60200000	13.11000000	15.57500000
C	22.21600000	11.71900000	16.52000000
C	24.18700000	13.01700000	15.74800000
C	26.17100000	14.34400000	15.14000000
C	21.43200000	12.88800000	16.31500000
C	23.36200000	14.13700000	15.44300000
C	25.32200000	15.44800000	14.83600000
C	21.95500000	14.05100000	15.71400000
C	23.95600000	15.33100000	14.96800000
H	23.34700000	16.20400000	14.73700000
H	22.20000000	4.94500000	17.14200000
O	24.67400000	5.92900000	17.47000000
C	22.04700000	5.66900000	17.95100000
C	24.02800000	6.97100000	17.36100000
H	22.53800000	5.28500000	18.85300000
N	22.63700000	6.96200000	17.58200000
C	24.63900000	8.26900000	16.99800000
H	20.98000000	5.82800000	18.12700000
C	21.78800000	8.07800000	17.45900000
O	20.57600000	7.98200000	17.64800000
C	22.43900000	9.35800000	17.08000000
C	21.66000000	10.48600000	16.94800000
H	20.59100000	10.39500000	17.14500000
S	19.77300000	13.10500000	16.76100000
C	20.96600000	15.06100000	15.55400000
C	19.74700000	14.73500000	16.10600000
H	21.15200000	16.01400000	15.07000000

O	29.38500000	15.90800000	14.44500000
C	4.53700000	17.70700000	17.35000000
C	4.07300000	16.76800000	18.39500000
H	3.58100000	15.01200000	20.08700000
N	5.07500000	16.08600000	19.11900000
C	4.66300000	15.14000000	20.16300000
C	6.45800000	16.24500000	18.92900000
O	7.25600000	15.59400000	19.60600000
H	4.92900000	15.53400000	21.15300000
H	5.18700000	14.18900000	20.02000000
H	4.64600000	22.44000000	11.73700000
C	5.34900000	21.87000000	12.34400000
H	3.84300000	21.06200000	13.62100000
C	4.91100000	21.08900000	13.40900000
H	3.23300000	19.77700000	15.00200000
C	7.64000000	21.21100000	12.79400000
C	5.80600000	20.34800000	14.20300000
C	4.00100000	19.26900000	15.58200000
C	7.20100000	20.42600000	13.90400000
C	5.36100000	19.48100000	15.29000000
H	2.53600000	18.21800000	16.77900000
C	3.59300000	18.39600000	16.58500000
C	8.16500000	19.72100000	14.68900000
C	6.33900000	18.78500000	16.06900000
C	9.54500000	19.79000000	14.33600000
C	7.73700000	18.92300000	15.79900000
C	5.91100000	17.90500000	17.10800000
C	10.46800000	19.04200000	15.12100000
C	8.68500000	18.22300000	16.60100000
C	6.88000000	17.20300000	17.88200000
C	10.07800000	18.30700000	16.26000000
C	8.22600000	17.38100000	17.64300000
H	8.92700000	16.81500000	18.25500000
H	8.46200000	23.19100000	8.51700000
O	6.37100000	23.41200000	10.18100000
C	8.94800000	23.56200000	9.42800000
C	7.14800000	22.75200000	10.87100000
H	8.64500000	24.60500000	9.57800000
N	8.52700000	22.75400000	10.58000000
C	6.70700000	21.93100000	12.02100000
H	10.03400000	23.48100000	9.34400000
C	9.51000000	22.04800000	11.30100000
O	10.69700000	22.09200000	10.98000000
C	9.02800000	21.25700000	12.46200000

C	9.94500000	20.56000000	13.21400000
H	10.99500000	20.61900000	12.92400000
S	12.15400000	18.82400000	14.77800000
C	11.17500000	17.61000000	16.84800000
C	12.35000000	17.75000000	16.14700000
H	11.09500000	16.96800000	17.72100000
O	2.88000000	16.57200000	18.62700000
C	4.52300000	14.73200000	15.37800000
C	4.01400000	15.67300000	14.35900000
H	3.69900000	17.91300000	12.99500000
N	4.97700000	16.35500000	13.58700000
C	4.46200000	17.26200000	12.55500000
C	6.37200000	16.21400000	13.72000000
O	7.15100000	16.85900000	13.01700000
H	3.99700000	16.68400000	11.74500000
H	5.30200000	17.84400000	12.16900000
H	4.90100000	9.58100000	20.59800000
C	5.57300000	10.21900000	20.02500000
H	4.00400000	11.16100000	18.92500000
C	5.08100000	11.11300000	19.07900000
H	3.33300000	12.62200000	17.75000000
C	7.83800000	10.92700000	19.52800000
C	5.93700000	11.93300000	18.31900000
C	4.07100000	13.13400000	17.13600000
C	7.34500000	11.82800000	18.53500000
C	5.44200000	12.88600000	17.33000000
H	2.55300000	14.23200000	16.05300000
C	3.61800000	14.04000000	16.18300000
C	8.26900000	12.60800000	17.77500000
C	6.38300000	13.61800000	16.53900000
C	9.66300000	12.51800000	18.05900000
C	7.79000000	13.47900000	16.74400000
C	5.90700000	14.53200000	15.55100000
C	10.54300000	13.35100000	17.31500000
C	8.70100000	14.23400000	15.94800000
C	6.83900000	15.25800000	14.75200000
C	10.10300000	14.16300000	16.24900000
C	8.19400000	15.09900000	14.94600000
H	8.86800000	15.68600000	14.32400000
H	8.86200000	8.39700000	23.45500000
O	6.70800000	8.41200000	21.90900000
C	9.32100000	8.16800000	22.48500000
C	7.44700000	9.15800000	21.26700000
H	9.03300000	7.14800000	22.20300000

N	8.84000000	9.11700000	21.47400000
C	6.94600000	10.12000000	20.26000000
H	10.40800000	8.26200000	22.53900000
C	9.78300000	9.90900000	20.79200000
O	10.98600000	9.81900000	21.03000000
C	9.24100000	10.84300000	19.77400000
C	10.11900000	11.63200000	19.06700000
H	11.18300000	11.54200000	19.29200000
S	12.22800000	13.58700000	17.63600000
C	11.16600000	14.93300000	15.69200000
C	12.36000000	14.77200000	16.35500000
H	11.04700000	15.62900000	14.86700000
O	2.81400000	15.87200000	14.16800000
H	14.82100000	18.75800000	16.35300000
H	17.29900000	18.73300000	16.57600000
H	14.82700000	13.78200000	16.20500000
H	17.28100000	13.79700000	16.04900000

Reference

1. Liu, J.; Chen, S. S.; Qian, D. P.; Gautam, B.; Yang, G. F.; Zhao, J. B.; Bergqvist, J.; Zhang, F. L.; Ma, W.; Ade, H.; Inganas, O.; Gundogdu, K.; Gao, F.; Yan, H., Fast charge separation in a non-fullerene organic solar cell with a small driving force. *Nat. Energy* **2016,** *1* (7), 16089.

2. Zhang, H.; Lin, H.; Sun, K.; Chen, L.; Zagranyarski, Y.; Aghdassi, N.; Duhm, S.; Li, Q.; Zhong, D.; Li, Y.; Mullen, K.; Fuchs, H.; Chi, L., On-surface synthesis of rylene-type graphene nanoribbons. *J. Am. Chem. Soc.* **2015,** *137* (12), 4022-5.

3. Carlotti, B.; Cai, Z.; Kim, H.; Sharapov, V.; Madu, I. K.; Zhao, D.; Chen, W.; Zimmerman, P. M.; Yu, L.; Goodson, T., Charge Transfer and Aggregation Effects on the Performance of Planar vs Twisted Nonfullerene Acceptor Isomers for Organic Solar Cells. *Chem. Mater.* **2018,** *30* (13), 4263-4276.

4. Wang, X.; Yan, J.; Zhou, Y.; Pei, J., Surface modification of self-assembled one-dimensional organic structures: white-light emission and beyond. *J. Am. Chem. Soc.* **2010,** *132* (45), 15872-4.

5. Hexemer, A.; Bras, W.; Glossinger, J.; Schaible, E.; Gann, E.; Kirian, R.; MacDowell, A.; Church, M.; Rude, B.; Padmore, H., A SAXS/WAXS/GISAXS Beamline with Multilayer Monochromator. *Journal of Physics: Conference Series* **2010,** *247*.

6. Ilavsky, J., Nika: software for two-dimensional data reduction. *Journal of Applied Crystallography* **2012,** *45* (2), 324-328.

7. Gann, E.; Young, A. T.; Collins, B. A.; Yan, H.; Nasiatka, J.; Padmore, H. A.; Ade, H.; Hexemer, A.; Wang, C., Soft x-ray scattering facility at the Advanced Light Source with real-time data processing and analysis. *Rev Sci Instrum* **2012,** *83* (4), 045110.

8. VandeVondele, J.; Krack, M.; Mohamed, F.; Parrinello, M.; Chassaing, T.; Hutter, J., Quickstep: Fast and accurate density functional calculations using a mixed Gaussian and plane waves approach. *Computer Physics Communications* **2005,** *167* (2), 103-128.

9. VandeVondele, J.; Hutter, J., Gaussian basis sets for accurate calculations on molecular systems in gas and condensed phases. *J Chem Phys* **2007,** *127* (11), 114105.
10. Goedecker, S.; Teter, M.; Hutter, J., Separable dual-space Gaussian pseudopotentials. *Physical Review B* **1996,** *54* (3), 1703.
11. Perdew, J. P.; Burke, K.; Ernzerhof, M., Generalized gradient approximation made simple. *Physical Review Letters* **1996,** *77* (18), 3865-3868.
12. Grimme, S.; Antony, J.; Ehrlich, S.; Krieg, H., A consistent and accurate ab initio parametrization of density functional dispersion correction (DFT-D) for the 94 elements H-Pu. *J Chem Phys* **2010,** *132* (15), 154104.
13. Genovese, L.; Deutsch, T.; Neelov, A.; Goedecker, S.; Beylkin, G., Efficient solution of Poisson's equation with free boundary conditions. *The Journal of chemical physics* **2006,** *125* (7), 074105.